

Cite this: *Chem. Sci.*, 2023, **14**, 8869

All publication charges for this article have been paid for by the Royal Society of Chemistry

Received 6th June 2023  
Accepted 12th July 2023

DOI: 10.1039/d3sc02868b  
[rsc.li/chemical-science](http://rsc.li/chemical-science)

## Thiol-triggered deconstruction of bifunctional silyl ether terpolymers via an $S_NAr$ -triggered cascade†

Christopher M. Brown,<sup>ID</sup><sup>a</sup> Keith E. L. Husted,<sup>a</sup> Yuyan Wang,<sup>a</sup> Landon J. Kilgallon,<sup>a</sup> Peyton Shieh,<sup>a</sup> Hadiqa Zafar,<sup>ID</sup><sup>a</sup> David J. Lundberg<sup>ab</sup> and Jeremiah A. Johnson<sup>ID</sup><sup>\*ac</sup>

While Si-containing polymers can often be deconstructed using chemical triggers such as fluoride, acids, and bases, they are resistant to cleavage by mild reagents such as biological nucleophiles, thus limiting their end-of-life options and potential environmental degradability. Here, using ring-opening metathesis polymerization, we synthesize terpolymers of (1) a “functional” monomer (e.g., a polyethylene glycol macromonomer or dicyclopentadiene); (2) a monomer containing an electrophilic pentafluorophenyl (PFP) substituent; and (3) a cleavable monomer based on a bifunctional silyl ether ( $SiR_2(OR'_2)$ ). Exposing these polymers to thiols under basic conditions triggers a cascade of nucleophilic aromatic substitution ( $S_NAr$ ) at the PFP groups, which liberates fluoride ions, followed by cleavage of the backbone Si–O bonds, inducing polymer backbone deconstruction. This method is shown to be effective for deconstruction of polyethylene glycol (PEG) based graft terpolymers in organic or aqueous conditions as well as polydicyclopentadiene (pDCPD) thermosets, significantly expanding upon the versatility of bifunctional silyl ether based functional polymers.

## Introduction

Polymers that undergo selective bond cleavage<sup>1</sup> in response to an external trigger have numerous applications, including in drug delivery,<sup>2–4</sup> sensing,<sup>5,6</sup> transient electronics,<sup>7,8</sup> and recyclable materials.<sup>9,10</sup> A wide range of functional groups (e.g., azo,<sup>11–13</sup> dihydrofuran,<sup>14</sup> disulfide,<sup>15,16</sup> diselenium,<sup>17</sup> ester,<sup>18</sup> ketal,<sup>19</sup> poly(benzyl ether),<sup>20</sup> and phosphoramidate<sup>21</sup>) have been employed to enable triggered polymer deconstruction, and various external stimuli such as oxidation/reduction,<sup>22,23</sup> pH,<sup>24,25</sup> light,<sup>12</sup> heat,<sup>26</sup> nucleophiles,<sup>27</sup> and mechanical force<sup>28</sup> have been extensively studied. Nevertheless, there is often a trade-off between the introduction of cleavable bonds and polymer stability under use conditions, especially when mild cleavage reagents (e.g., biological triggers), and thus easier-to-cleave bonds, are required.

Bifunctional silyl ethers ( $SiR_2(OR'_2)$ ; “BSEs”) are versatile functional groups that have found applications as fluoride- and acid/base-cleavable linkages in, for example, biomaterials,<sup>29</sup> controlled release systems,<sup>30–32</sup> and deconstructable thermosets (Fig. 1A).<sup>33–37</sup> BSEs offer a unique combination of synthetic

accessibility, compositional diversity,<sup>38</sup> and excellent thermal and oxidative stabilities while providing for highly selective cleavage with rates that can be easily controlled through variation of the Si–R substituents.<sup>39</sup> Moreover, cyclic olefins containing BSEs are suitable monomers for the synthesis of deconstructable homopolymers,<sup>40</sup> copolymers,<sup>39</sup> and thermosets via ring-opening metathesis polymerization (ROMP).<sup>35–38,41</sup> Nevertheless, while acid and/or fluoride are convenient triggers for BSE cleavage, there are instances where such stimuli are not compatible with a desired application, leading us to consider alternative methods.

Inspired by advances in radical ring-opening polymerization—where sensitive electrophilic functional groups such as thioesters can be installed within polymer backbones to enable cleavage via nucleophilic attack<sup>27,42,43</sup>—and with interest in biodegradable polymers, we sought a strategy to facilitate the deconstruction of BSE-based polymers prepared via ROMP through exposure to nucleophiles such as thiols. While BSEs are not sufficiently reactive to undergo cleavage in the presence of thiols under typical conditions, we hypothesized that it would be possible to embed latent, thiol-triggered fluoride sources into BSE-containing polymers to facilitate Si–O bond cleavage following a nucleophilic aromatic substitution ( $S_NAr$ ) event.  $S_NAr$  reactions of pentafluorophenyl (PFP) derivatives<sup>44</sup> using a range of nucleophiles (e.g., alcohols,<sup>45</sup> amines,<sup>46</sup> phosphites,<sup>47</sup> thiols<sup>44,48,49</sup>) liberate one equivalent of  $F^-$  per substitution reaction, which we imagined could be utilized as the first step in an  $S_NAr$ , fluoride release, and BSE cleavage cascade (Fig. 1B). Additionally,  $S_NAr$  reactions of PFP groups are known to be

<sup>a</sup>Department of Chemistry, Massachusetts Institute of Technology, 77 Massachusetts Avenue, Cambridge, MA 02139, USA. E-mail: [jaj2109@mit.edu](mailto:jaj2109@mit.edu)

<sup>b</sup>Department of Chemical Engineering, Massachusetts Institute of Technology, 77 Massachusetts Avenue, Cambridge, MA 02139, USA

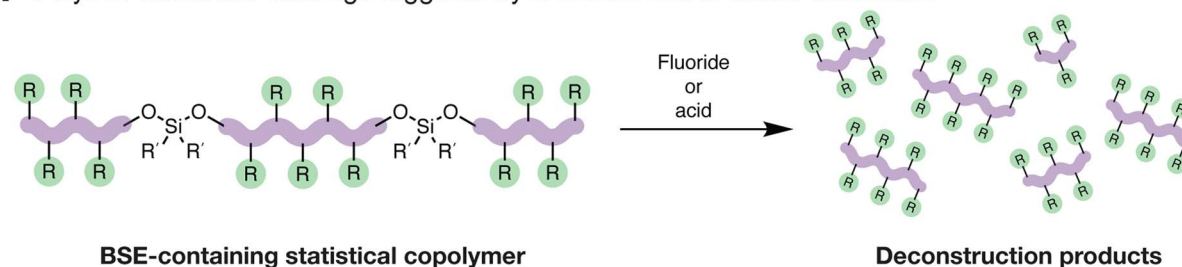
<sup>c</sup>David H. Koch Institute for Integrative Cancer Research, Massachusetts Institute of Technology, 77 Massachusetts Avenue, Cambridge, Massachusetts 02139, USA

† Electronic supplementary information (ESI) available. See DOI: <https://doi.org/10.1039/d3sc02868b>



## Previous work:

## A Polymer backbone cleavage triggered by a fluoride salt or acidic conditions



## This work:

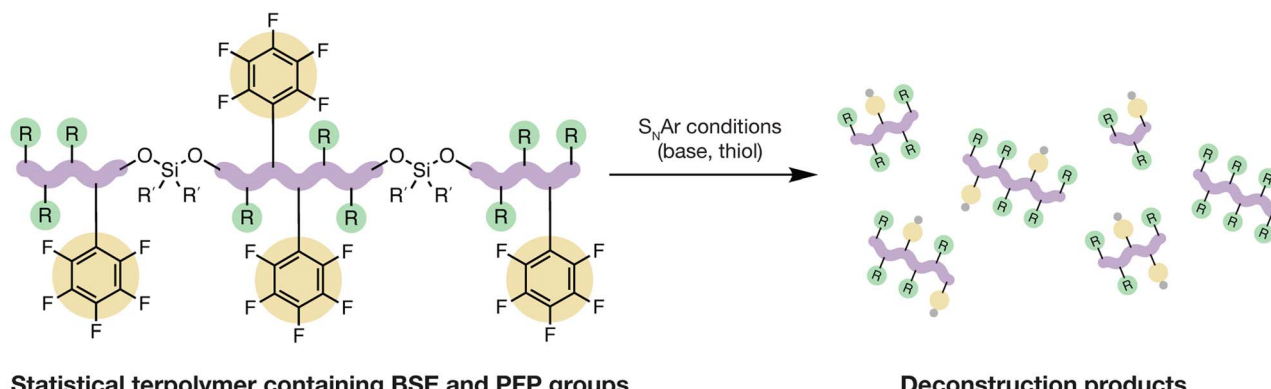
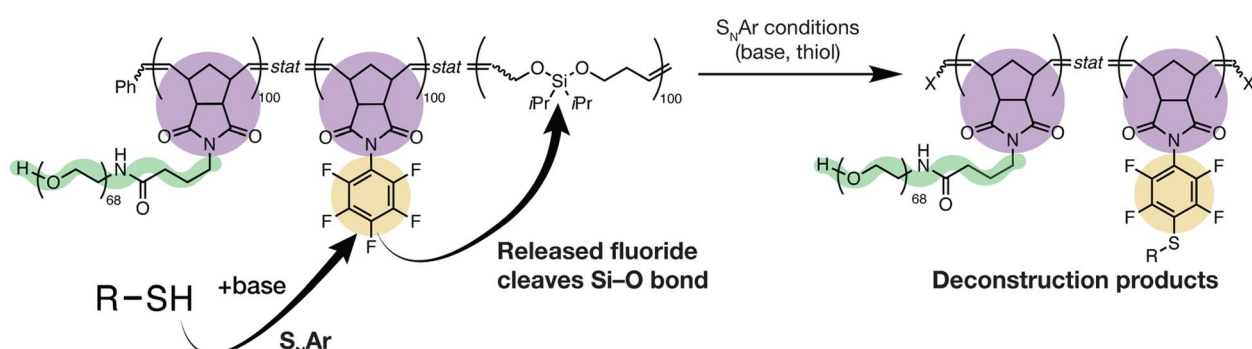
B Polymer backbone cleavage *via* S<sub>N</sub>Ar-induced fluoride releaseC S<sub>N</sub>Ar-mediated deconstruction proceeds *via* a cascade reaction

Fig. 1 (A) We have previously reported deconstructable copolymers containing bifunctional silyl ethers (BSEs) where polymer backbone cleavage is initiated by a fluoride source (e.g., tetrabutylammonium fluoride, TBAF) or acidic conditions (e.g., HCl or carboxylic acids), providing oligomeric deconstruction fragments. (B) Here, we describe BSE-containing terpolymers containing pentafluorophenyl (PFP) comonomers, which trigger deconstruction upon exposure to nucleophilic aromatic substitution (S<sub>N</sub>Ar) conditions (a thiol in the presence of base). (C) The S<sub>N</sub>Ar-mediated cleavage proceeds *via* a cascade reaction, where thiolate attacks at the *para*-position of the PFP ring *via* S<sub>N</sub>Ar, releasing a fluoride ion, which in turn cleaves the Si-O bond of the BSE. At full conversion, X = CH<sub>2</sub>CH<sub>2</sub>OH, CH<sub>2</sub>OH, Ph or H.

effective reactions for polymer functionalization.<sup>50-54</sup> PFPs are compatible with ROMP, and there are many cheap, benign, and/or biologically-derived thiols that could potentially be used to initiate such a cascade process. Here, we present the realization of this concept, showing that graft and covalently crosslinked thermoset terpolymers with BSE- and PFP-based comonomers

undergo selective backbone cleavage *via* a thiol-triggered S<sub>N</sub>Ar cascade. This work provides a new strategy to enable backbone cleavage of otherwise stable polymeric materials and extends the scope of BSE-based cleavage reactions for responsive materials design.



## Results and discussion

### Small molecule model studies

First, we sought to determine whether or not BSEs are stable under typical conditions used for  $S_NAr$  reactions involving PFP groups, which often involve polar organic solvents and bases such as  $K_2CO_3$ ,  $Cs_2CO_3$  or 1,8-diazabicyclo[5.4.0]undec-7-ene (DBU).<sup>44</sup> PFP-based monomer **Nb-PFP** (synthesized following a reported procedure<sup>55</sup>) and **iPrAl**, a BSE mimic of a polymer backbone, were exposed to various conditions relevant to  $S_NAr$  (Fig. 2A); gas chromatography-mass spectrometry (GC-MS) was used to monitor **iPrAl** cleavage (mesitylene was used as an internal standard; see ESI† section “Small Molecule GC-MS Studies” for further information; see ESI† section “Small molecule syntheses” for details). **iPrAl** remained intact when treated with either 1-dodecanethiol (nucleophile, 1.5 equiv.),  $K_2CO_3$  (base, 2.0 equiv.), **Nb-PFP** (latent fluoride, 1.5 equiv.), a combination of 1-dodecanethiol and  $K_2CO_3$  (nucleophile and base only), or with a combination of **Nb-PFP** and  $K_2CO_3 (latent fluoride and base) (Fig. 2B). When **iPrAl** was exposed to 1-dodecanethiol (1.5 equiv.),  $K_2CO_3$  (2.0 equiv.), and **Nb-PFP** (1.5 equiv., *i.e.*, all three reagents critical for  $S_NAr$ ), however, >98% cleavage was observed after 1 h and no trace of **iPrAl** was seen after 2 h (Fig. S1†).  $^{19}F$  NMR spectroscopy of the reaction mixture showed a doublet of doublets of doublets and a multiplet with a downfield shift when compared to the parent **Nb-PFP** (Fig. S2A†). This spectrum agrees well with the spectrum obtained for an independently synthesized, authentic sample of the expected *para*-1-dodecanethiol-substituted product **Nb-PFP-SC<sub>12</sub>H<sub>25</sub>** (see ESI† section “Small molecule syntheses” for details). Moreover, a  $^{19}F$ - $^{19}F$  COSY experiment showed a correlation between the two new  $^{19}F$  resonances generated under the reaction conditions (Fig. S2B†). Altogether, these results confirm that  $S_NAr$  occurs between 1-dodecanethiol and **Nb-PFP** in the presence of  $K_2CO_3$ , and that the resulting fluoride can cleave a model BSE.$

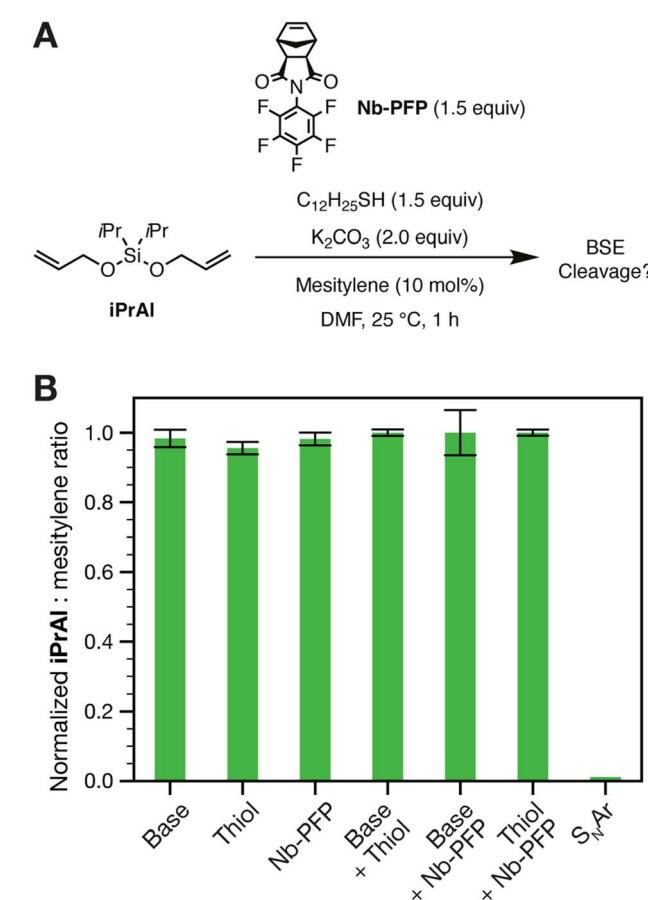


Fig. 2 (A) Scheme showing the methodology for the small molecule GC-MS studies of acyclic BSE*i*PrAl. (B) Bar chart comparing the ratio of *i*PrAl to a mesitylene internal standard (10 mol%) from GC-MS runs. *i*PrAl is treated with either  $K_2CO_3$  (base), **Nb-PFP**, 1-dodecanethiol (thiol), or combinations of the above in DMF for 1 h at 25 °C. Ratios were calculated using peak integration and averaged over three runs. Error bars show standard deviation.

equiv., *i.e.*, all three reagents critical for  $S_NAr$ ), however, >98% cleavage was observed after 1 h and no trace of **iPrAl** was seen after 2 h (Fig. S1†).  $^{19}F$  NMR spectroscopy of the reaction mixture showed a doublet of doublets of doublets and a multiplet with a downfield shift when compared to the parent **Nb-PFP** (Fig. S2A†). This spectrum agrees well with the spectrum obtained for an independently synthesized, authentic sample of the expected *para*-1-dodecanethiol-substituted product **Nb-PFP-SC<sub>12</sub>H<sub>25</sub>** (see ESI† section “Small molecule syntheses” for details). Moreover, a  $^{19}F$ - $^{19}F$  COSY experiment showed a correlation between the two new  $^{19}F$  resonances generated under the reaction conditions (Fig. S2B†). Altogether, these results confirm that  $S_NAr$  occurs between 1-dodecanethiol and **Nb-PFP** in the presence of  $K_2CO_3$ , and that the resulting fluoride can cleave a model BSE.

### Nb-PFP homopolymer model studies

To test the viability of  $S_NAr$  in a ROMP-derived PFP-containing polymer, we subjected **Nb-PFP** (225 equiv.) to Grubbs' 3rd generation bispyridyl initiator (1 equiv.) in 1,4-dioxane, providing **PolyNb-PFP** (Fig. 3A, see ESI† section “Polymer syntheses” for details). The  $^1H$  NMR spectrum of **PolyNb-PFP** agrees well with that reported by Tlenkopatchev and coworkers for similar polymers synthesized using Grubbs 1st and 2nd-generation initiators.<sup>56</sup> Complete consumption of **Nb-PFP** was observed (Fig. S3†).  $^{19}F$  NMR showed the same three general sets of resonances for **PolyNb-PFP** and **Nb-PFP** (Fig. S4†). **PolyNb-PFP** had a low dispersity ( $D = 1.05$ ) and a number average molecular weight ( $M_n$ ) of 78 400, close to its theoretical  $M_n$  of 74 100, as determined by size exclusion chromatography (SEC,  $CHCl_3$  mobile phase) (Fig. 3B, black trace). Exposure of **PolyNb-PFP** to C<sub>12</sub>H<sub>25</sub>SH (1.2 equiv.) and  $K_2CO_3$  (2.0 equiv.) in DMF at 25 °C (Fig. 3C, see ESI† section “Polymer syntheses” for details) for 1 h gave quantitative conversion to the *para*-substituted  $S_NAr$  product as determined by  $^{19}F$  NMR spectroscopy (Fig. 3D). SEC ( $CHCl_3$  mobile phase) showed a concomitant increase in molecular weight ( $M_n$  of 123 800, close to its theoretical  $M_n$  of 115 100) and slight increase in dispersity ( $D = 1.15$ ) (Fig. 3B). A small shoulder is observed, which we attribute to aggregation of the substituted polymer, likely caused by the addition of dodecyl groups to the polymer sidechains.

### Terpolymer deconstruction using an $S_NAr$ -initiated cascade

After successfully demonstrating  $S_NAr$  of **PolyNb-PFP**, we set out to test our hypothesis that an  $S_NAr$ -triggered cascade can enable deconstruction of polymers with backbone BSE groups. **Nb-PFP** was combined with BSE-containing monomer **iPrSi8** (synthesized according to a reported procedure<sup>39</sup>) and norbornene-terminated 3 kDa polyethylene glycol (PEG) macromonomer<sup>57</sup> **PEG-MM** in a 1 : 1 : 1 molar ratio in 1,4-dioxane and exposed to Grubbs' 3rd-generation bis-pyridyl initiator to generate graft terpolymer **P1** (total monomer : initiator ratio 300 : 1) (Fig. 4A, see ESI† section “Polymer syntheses” for experimental details). High conversions of **iPrSi8**, **Nb-PFP** and **PEG-MM** were confirmed *via*  $^1H$  NMR (Fig. S5†) and  $^{19}F$  NMR spectroscopy (Fig. S6†) to yield **P1** with  $M_n$  of 636 000 ( $\pm 18.6\%$ ) and  $D = 1.57$  (See ESI† section “Materials and Methods” for

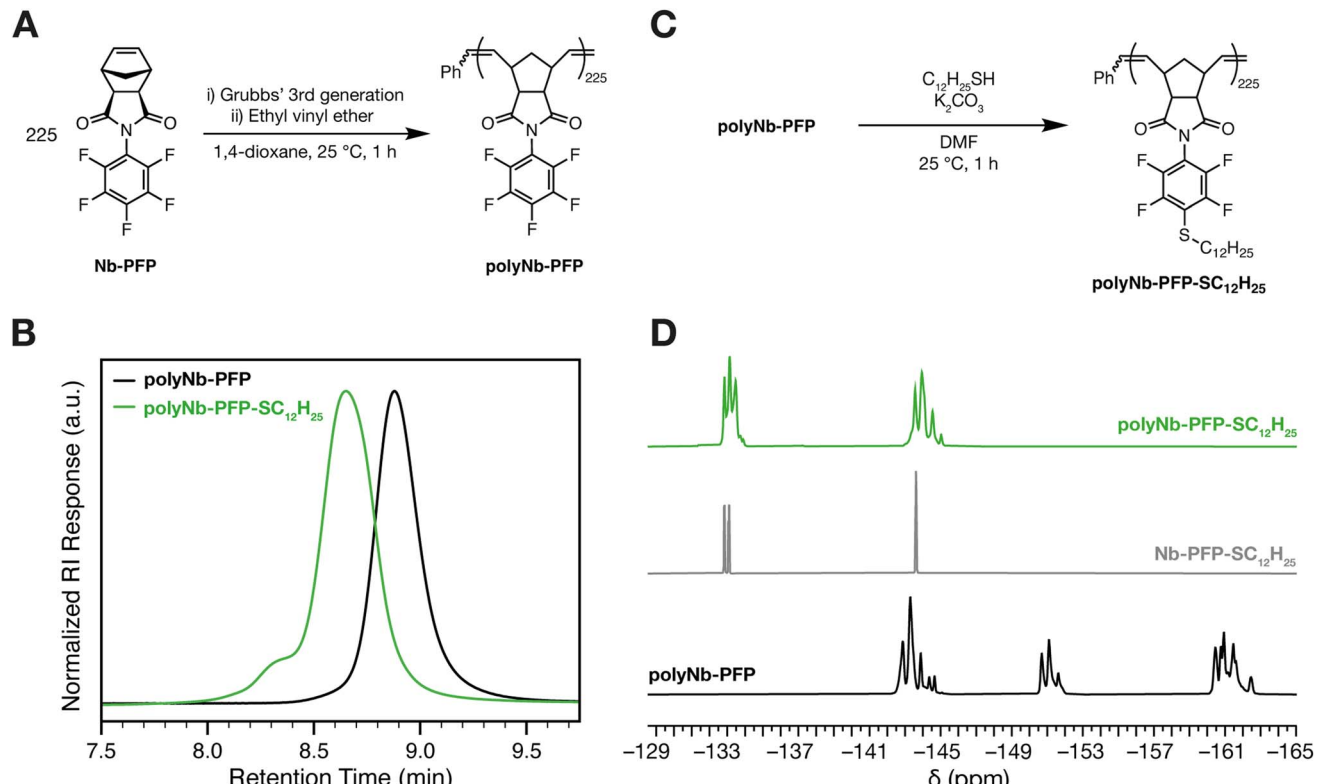


Fig. 3 (A) Synthesis of polyNb-PFP homopolymer. (B) SEC traces ( $\text{CHCl}_3$  mobile phase) for polyNb-PFP (black) and  $\text{S}_{\text{NAr}}$  product polyNb-PFP- $\text{SC}_{12}\text{H}_{25}$ . (C) Synthesis of  $\text{S}_{\text{NAr}}$  product polyNb-PFP- $\text{SC}_{12}\text{H}_{25}$ . (D)  $^{19}\text{F}$  NMR spectra (565 MHz,  $\text{CDCl}_3$ , 25 °C) comparing polyNb-PFP (black) to monomer Nb-PFP- $\text{SC}_{12}\text{H}_{25}$  (grey) and polyNb-PFP- $\text{SC}_{12}\text{H}_{25}$  (green).

a discussion on  $M_n$  calculations). To confirm that BSEs are incorporated into the polymer backbone, **P1** was exposed to 1 M aqueous HCl (see ESI† section “Degradation studies” for experimental details), conditions previously shown to cleave BSEs in norbornene-based terpolymers.<sup>39</sup> SEC analysis revealed macromolecular deconstruction products at longer retention times, indicative of polymer backbone cleavage resulting in monomers, dimers, trimers, and higher oligomers<sup>39</sup> (Fig. 4B). Moreover,  $^{19}\text{F}$  NMR spectroscopy shows that the PFP group remains unaffected under these conditions (Fig. 4C).

Gratifyingly, exposure of **P1** to  $\text{S}_{\text{NAr}}$  conditions— $\text{K}_2\text{CO}_3$  (2.0 equiv. w.r.t. Nb-PFP in the terpolymer) and 1-dodecanethiol (1.5 equiv. w.r.t. Nb-PFP in the terpolymer) in DMF—for 30 min at 25 °C led to backbone deconstruction and a nearly identical SEC trace to that for HCl-induced deconstruction (Fig. 4B, purple trace; see ESI† section “Deconstruction studies” for experimental details).  $^{19}\text{F}$  NMR spectroscopy confirms formation of the expected  $\text{S}_{\text{NAr}}$  product, suggesting that deconstruction is triggered by  $\text{S}_{\text{NAr}}$  (Fig. 4C). Notably, exposing the polymer to  $\text{K}_2\text{CO}_3$  alone (in DMF at room temperature) for the same time period does not lead to any polymer cleavage by SEC (Fig. 4B, green trace,  $M_n = 536\,000$  ( $\pm 17.1\%$ ),  $D = 1.53$ ); exposing the polymer to 1-dodecanethiol in the absence of base leads to a small shift in the SEC peak to a longer retention time, suggesting a small amount of decomposition likely due to background  $\text{S}_{\text{NAr}}$  (Fig. 4B, yellow trace,  $M_n = 268\,000$  ( $\pm 14.6\%$ ),  $D = 1.57$ ).

#### PEG-based graft terpolymer deconstruction under aqueous conditions

We initially designed **iPrSi8** and related monomers<sup>39</sup> for the purpose of enabling the deconstruction of PEG-based graft terpolymers under aqueous conditions that may be translatable to applications in drug delivery and biological imaging.<sup>58–62</sup> Delaittre and coworkers reported thiol-mediated  $\text{S}_{\text{NAr}}$  of PFP-containing poly(*N,N*-dimethylacrylamide) in alkaline water ( $\text{pH} \geq 11$ ),<sup>63</sup> which inspired us to investigate backbone deconstruction of **P1** under similar conditions. First, we exposed the polymer to  $\text{Na}_2\text{HPO}_4$ /NaOH buffer solution ( $\text{pH} = 12$ ; see ESI† section “Degradation studies” for full experimental details) for 30 min at 25 °C; very little change was observed by SEC following this treatment, suggesting that the polymer is stable in aqueous alkaline buffer (Fig. S7†). When 2-mercaptoethanol (1.5 equiv. per PFP group) was added to this solution, which is sufficiently basic to generate the corresponding thiolate ( $\text{pK}_a$  of 2-mercaptoethanol = 9.72),<sup>64</sup> complete polymer deconstruction was observed in 30 min at room temperature (Fig. 5).  $^{19}\text{F}$  NMR spectroscopy confirms the formation of  $\text{S}_{\text{NAr}}$  products, consistent with  $\text{S}_{\text{NAr}}$ -induced fluoride release and BSE cleavage (Fig. S8†). The efficiency of this reaction is notable; previous work suggested that elevated temperatures (e.g., 40 °C), extend reaction times (e.g., 72 h), and large excesses of thiols (e.g., 10–20 equiv.) are needed to induce  $\text{S}_{\text{NAr}}$  of polymeric PFP groups under aqueous conditions.<sup>63</sup> Here, deconstruction may be facilitated by the



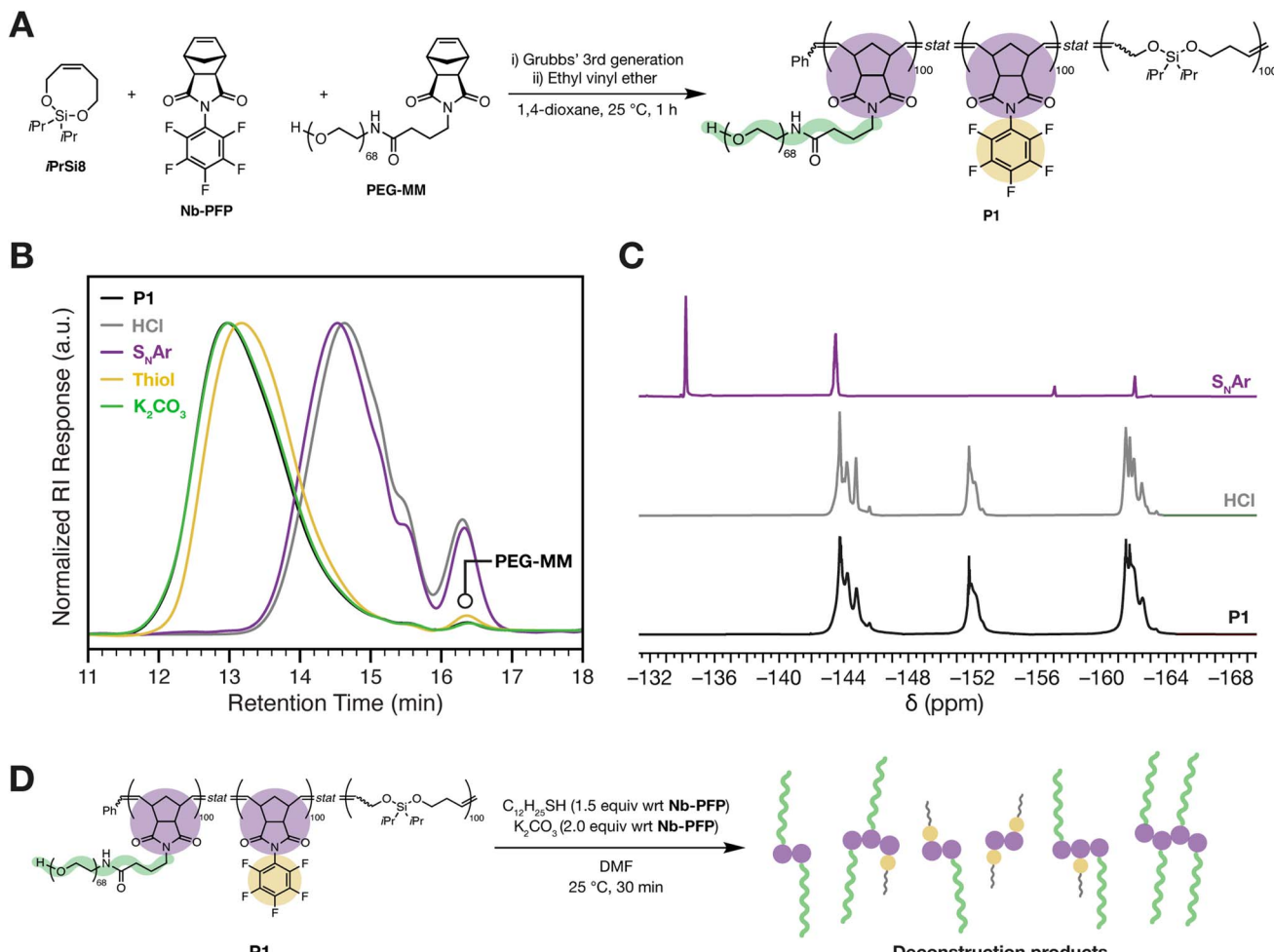


Fig. 4 (A) Synthesis of polynorbornene graft terpolymer **P1** via ROMP. Incorporation of PEG-MM into the terpolymer enables facile tracking of subsequent deconstruction. (B) SEC traces (DMF mobile phase) showing polymer **P1** (black), the control deconstruction of **P1** using HCl (grey), the control deconstruction of **P1** using  $\text{K}_2\text{CO}_3$  (green), the control deconstruction of **P1** using 1-dodecanethiol (thiol, yellow) and the deconstruction of **P1** using the  $\text{S}_\text{NAr}$  conditions of 1-dodecanethiol and  $\text{K}_2\text{CO}_3$  (purple). (C)  ${}^{19}\text{F}$  NMR spectra (565 MHz,  $\text{CDCl}_3$ , 25  $^{\circ}\text{C}$ ) comparing the parent terpolymer **P1** (black), to the deconstruction products using HCl (grey), or  $\text{S}_\text{NAr}$  conditions (purple). (D) Schematic showing the deconstruction of **P1** using  $\text{S}_\text{NAr}$  conditions.

hydrophobic local environment of **P1**, where the PFP and BSE groups reside, which may elevate the local concentration of thiol and/or stabilize the  $\text{S}_\text{NAr}$  transition state.

#### Thiol-triggered cascade deconstruction of polydicyclopentadiene thermosets

We have shown that BSE-containing monomers such as **iPrSi8** can be copolymerized with dicyclopentadiene (DCPD) to generate deconstructable<sup>38,41</sup> and remoldable<sup>35</sup> polydicyclopentadiene (pDCPD) thermosets and composites, offering a new end-of-life strategy for this high-performance engineering material.<sup>65</sup> Nevertheless, in these studies we have used 1 M TBAF, 1 M HCl, or high-temperature treatment with octanoic acid as deconstruction triggers; we hypothesized that the  $\text{S}_\text{NAr}$ -triggered cascade process introduced here could serve as an alternative method for pDCPD deconstruction.

To test this hypothesis, we prepared two thermosets: the first—thermoset **T1** (Fig. 6A)—was prepared by curing a liquid

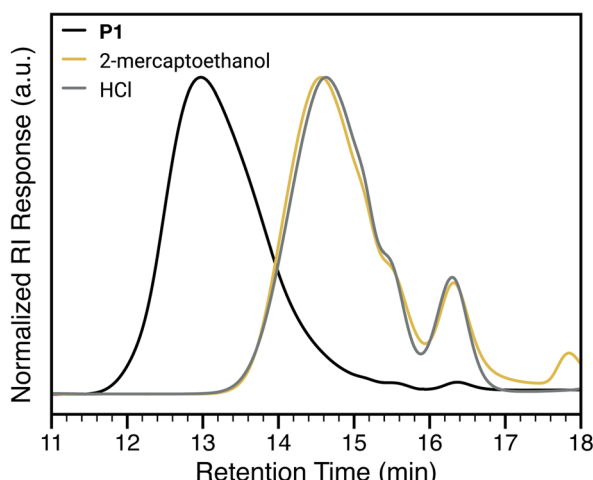
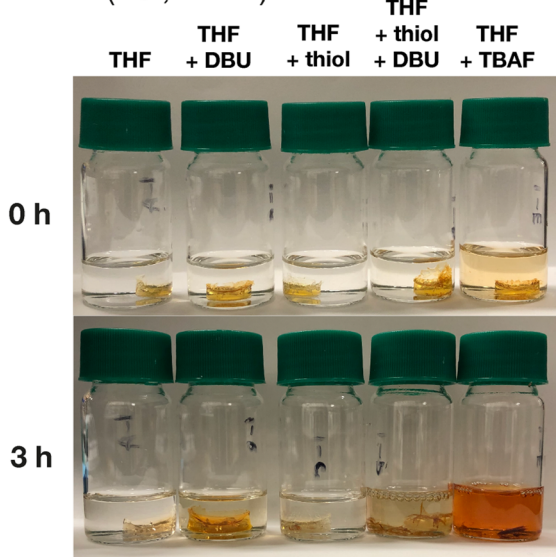
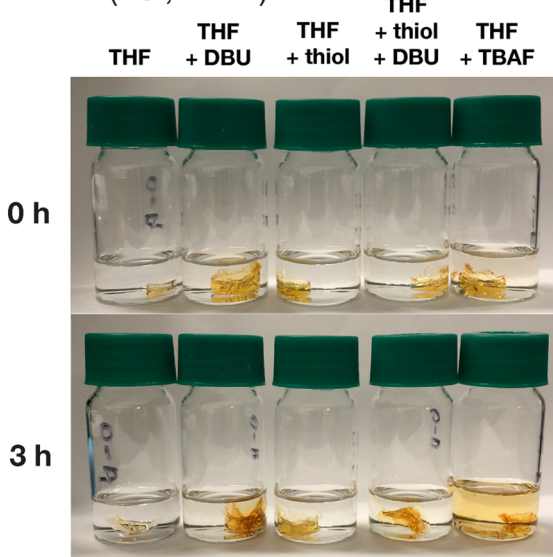


Fig. 5 Deconstruction of **P1** in pH 12 buffer. SEC traces (DMF mobile phase) of the parent terpolymer (black), HCl-deconstructed material (grey), and **P1** exposed to 2-mercaptoethanol in pH 12  $\text{Na}_2\text{HPO}_4/\text{NaOH}$  buffer solution (yellow).

**A T1 (+Si, +PFP)****B T2 (+Si, -PFP)**

**Fig. 6** Deconstruction of BSE-containing pDCPD thermoset materials. (A) Thermoset **T1** (+Si, +PFP) prepared using pDCPD, iPrSi8 (10% v/v) and **Nb-PFP** (2.0 equiv. w.r.t. iPrSi8) in solutions of: THF; THF and DBU; THF and 1-dodecanethiol (thiol); THF, thiol, and DBU; THF and TBAF at 25 °C, after 0 and 3 h. (B) Control thermoset **T2** (+Si, -PFP) prepared using pDCPD and iPrSi8 (10% v/v) in solutions of: THF; THF and DBU; THF and 1-dodecanethiol (thiol); THF, thiol, and DBU; THF and TBAF at 25 °C, after 0 and 3 h.

resin containing DCPD (14.4 equiv.) with 10% v/v of **iPrSi8** (1.0 equiv.) and **Nb-PFP** (2.0 equiv.); the second—thermoset **T2** (Fig. 6B)—was prepared by curing a resin containing DCPD with 10% v/v of **iPrSi8** only (see ESI† section “Thermoset materials” for full experimental details). Two equivalents of **Nb-PFP** with respect to **iPrSi8** were chosen to facilitate full material deconstruction; as there are 2 Si–O bonds per BSE, 2 equiv. of fluoride are required to achieve complete Si–O bond cleavage. Dynamic mechanical analysis (DMA, Fig. S9 and Table S1†) showed that the glass transition temperature ( $T_g$ ) of **T1** ( $T_g = 67$  °C) was highly depressed compared to **T2** ( $T_g = 134$  °C), which is likely due to dilution of the thermoset crosslink density through incorporation of **Nb-PFP**. Nevertheless, thermogravimetric analysis (TGA, Fig. S10 and Table S2†) showed that the decomposition temperatures ( $T_d$ ) of **T1** ( $T_d = 458$  °C (plus a secondary shoulder at 550 °C due to addition of **Nb-PFP**)) and **T2** ( $T_d = 464$  °C) were similar, suggesting that the addition of **Nb-PFP** does not have a major negative impact on the stability of these two thermoset materials. The storage moduli ( $E'$ ) and loss moduli ( $E''$ ) of the thermosets were determined by DMA (Fig. S11 and S12,† respectively). **T1** and **T2** displayed similar  $E'$  at 30 °C (well below their respective  $T_g$  values) when compared to a neat pDCPD sample. Lower rubbery moduli (*i.e.*, moduli collected above  $T_g$ ) were observed for **Nb-PFP**-containing **T1** when compared to **T2** or neat pDCPD, which is also consistent with a reduced crosslink density.<sup>35</sup>

Both thermosets were exposed to  $S_NAr$  conditions,<sup>44</sup> in this case using 1-dodecanethiol (2.0 equiv. w.r.t. PFP groups) and the organic base 1,8-diazabicyclo[5.4.0]undec-7-ene (DBU, 2.0 equiv.) in tetrahydrofuran (THF) solvent, which facilitates swelling of the materials. In line with our hypothesis, **T1** was almost completely deconstructed (8% residual mass) to form soluble products

under these conditions (Fig. 6A) while **T2** remained intact (Fig. 6B). Both thermosets were dissolved in 1 M TBAF in THF (4% residual mass), confirming that the stability of **T2** under  $S_NAr$  conditions is due to a lack of latent fluoride groups. Moreover, **T1** did not dissolve in the presence of 1-dodecanethiol or DBU alone (Fig. S13–S16†). <sup>19</sup>F NMR analysis of the soluble fragments of **T1** deconstruction showed that under TBAF conditions (Fig. S17†), the three sets of resonances corresponding to the PFP group are retained and additional <sup>19</sup>F resonances consistent with difluorosilane cleavage products are observed,<sup>36</sup> in line with direct cleavage of the Si–O bond by TBAF. By contrast, fragments from  $S_NAr$  conditions show two downfield <sup>19</sup>F resonances (Fig. S18†), which is consistent with  $S_NAr$  of the PFP groups.

## Conclusions

In summary, we describe a new method to deconstruct BSE-containing macromolecules using thiol-mediated  $S_NAr$  of PFP groups, which liberates fluoride and induces Si–O bond cleavage. The method is shown to be applicable to soluble graft terpolymers and insoluble thermosets, and it works in organic (DMF and THF) solvents or water with an appropriate base ( $K_2CO_3$ , DBU, and phosphate buffer) and nucleophile (1-dodecanethiol and 2-mercaptoethanol). This approach expands the scope of BSE chemistry and may provide new ways to couple chemical triggers (*e.g.*, thiols) with polymer deconstruction to achieve novel functions and end-of-life options.

## Author contributions

CMB synthesized starting materials and polymers, performed GC-MS studies, and organic and aqueous degradation studies.



KELH and YW performed thermoset experiments. YW conducted DMA experiments, LJK synthesized fluorinated silyl ether analogues, PS synthesized iPrSi8, HZ performed GC-MS experiments, and DJL synthesized PEG-MM. CMB, PS and JAJ conceived of the project. CMB and JAJ wrote the manuscript.

## Conflicts of interest

CMB, PS and JAJ are named inventors on a patent application (US provisional application no. 63/195259) filed by the Massachusetts Institute of Technology on the monomers and copolymers in this work.

## Acknowledgements

This work was supported by the NSF Center for the Chemistry of Molecularly Optimized Networks (MONET, CHE-2116298). We thank Dr Mohanraja Kumar for assistance with GC-MS studies. CMB acknowledges the Natural Sciences and Engineering Research Council of Canada (NSERC) for a Postdoctoral Fellowship. PS acknowledges the American Cancer Society for a Postdoctoral Fellowship and DJL acknowledges support from the National Science Foundation (NSF) Graduate Research Fellowship Program.

## References

- 1 P. Shieh, M. R. Hill, W. Zhang, S. L. Kristufek and J. A. Johnson, Clip Chemistry: Diverse (Bio)(Macro) Molecular and Material Function through Breaking Covalent Bonds, *Chem. Rev.*, 2021, **121**(12), 7059–7121, DOI: [10.1021/acs.chemrev.0c01282](https://doi.org/10.1021/acs.chemrev.0c01282).
- 2 N. Kamaly, B. Yameen, J. Wu and O. C. Farokhzad, Degradable Controlled-Release Polymers and Polymeric Nanoparticles: Mechanisms of Controlling Drug Release, *Chem. Rev.*, 2016, **116**(4), 2602–2663, DOI: [10.1021/acs.chemrev.5b00346](https://doi.org/10.1021/acs.chemrev.5b00346).
- 3 P. Sharma, P. Negi and N. Mahindroo, Recent Advances in Polymeric Drug Delivery Carrier Systems, *Adv. Polym. Biomed. Appl.*, 2018, 369–388.
- 4 K. K. Bawa and J. K. Oh, Stimulus-Responsive Degradable Polylactide-Based Block Copolymer Nanoassemblies for Controlled/Enhanced Drug Delivery, *Mol. Pharm.*, 2017, **14**(8), 2460–2474, DOI: [10.1021/acs.molpharmaceut.7b00284](https://doi.org/10.1021/acs.molpharmaceut.7b00284).
- 5 E. S. Hosseini, S. Dervin, P. Ganguly and R. Dahiya, Biodegradable Materials for Sustainable Health Monitoring Devices, *ACS Appl. Bio Mater.*, 2021, **4**(1), 163–194, DOI: [10.1021/acsabm.0c01139](https://doi.org/10.1021/acsabm.0c01139).
- 6 M. E. Roth, O. Green, S. Gnaim and D. Shabat, Dendritic, Oligomeric, and Polymeric Self-Immobilative Molecular Amplification, *Chem. Rev.*, 2016, **116**(3), 1309–1352, DOI: [10.1021/acs.chemrev.5b00372](https://doi.org/10.1021/acs.chemrev.5b00372).
- 7 M. J. Tan, C. Owh, P. L. Chee, A. K. K. Kyaw, D. Kai and X. J. Loh, Biodegradable Electronics: Cornerstone for Sustainable Electronics and Transient Applications, *J. Mater. Chem. C*, 2016, **4**(24), 5531–5558, DOI: [10.1039/c6tc00678g](https://doi.org/10.1039/c6tc00678g).
- 8 X. Peng, K. Dong, Z. Wu, J. Wang and Z. L. Wang, A Review on Emerging Biodegradable Polymers for Environmentally Benign Transient Electronic Skins, *J. Mater. Sci.*, 2021, **56**(30), 16765–16789, DOI: [10.1007/s10853-021-06323-0](https://doi.org/10.1007/s10853-021-06323-0).
- 9 X. B. Lu, Y. Liu and H. Zhou, Learning Nature: Recyclable Monomers and Polymers, *Chem.-A Eur. J.*, 2018, **24**(44), 11255–11266, DOI: [10.1002/chem.201704461](https://doi.org/10.1002/chem.201704461).
- 10 M. Hong and E. Y. X. Chen, Chemically Recyclable Polymers: A Circular Economy Approach to Sustainability, *Green Chem.*, 2017, **19**(16), 3692–3706, DOI: [10.1039/c7gc01496a](https://doi.org/10.1039/c7gc01496a).
- 11 R. A. Kenley and G. E. Manser, Degradable Polymers. Incorporating a Difunctional Azo Compound into a Polymer Network To Produce Thermally Degradable Polyurethanes, *Macromolecules*, 1985, **18**(2), 127–131, DOI: [10.1021/ma00144a002](https://doi.org/10.1021/ma00144a002).
- 12 M. A. Ayer, S. Schrettl, S. Balog, Y. C. Simon and C. Weder, Light-Responsive Azo-Containing Organogels, *Soft Matter*, 2017, **13**(22), 4017–4023, DOI: [10.1039/c7sm00601b](https://doi.org/10.1039/c7sm00601b).
- 13 H. Mutlu, C. M. Geiselhart and C. Barner-Kowollik, Untapped Potential for Debonding on Demand: The Wonderful World of Azo-Compounds, *Mater. Horizons*, 2018, **5**(2), 162–183, DOI: [10.1039/c7mh00920h](https://doi.org/10.1039/c7mh00920h).
- 14 J. D. Feist, D. C. Lee and Y. Xia, A Versatile Approach for the Synthesis of Degradable Polymers via Controlled Ring-Opening Metathesis Copolymerization, *Nat. Chem.*, 2022, **14**(1), 53–58, DOI: [10.1038/s41557-021-00810-2](https://doi.org/10.1038/s41557-021-00810-2).
- 15 J. M. J. Paulusse, R. J. Amir, R. A. Evans and C. J. Hawker, Free Radical Polymers with Tunable and Selective Bio- and Chemical Degradability, *J. Am. Chem. Soc.*, 2009, **131**(28), 9805–9812, DOI: [10.1021/ja903245p](https://doi.org/10.1021/ja903245p).
- 16 Y. Tachibana, T. Baba and K. Kasuya, Environmental Biodegradation Control of Polymers by Cleavage of Disulfide Bonds, *Polym. Degrad. Stab.*, 2017, **137**, 67–74, DOI: [10.1016/j.polymdegradstab.2017.01.003](https://doi.org/10.1016/j.polymdegradstab.2017.01.003).
- 17 J. Xia, T. Li, C. Lu and H. Xu, Selenium-Containing Polymers: Perspectives toward Diverse Applications in Both Adaptive and Biomedical Materials, *Macromolecules*, 2018, **51**(19), 7435–7455, DOI: [10.1021/acs.macromol.8b01597](https://doi.org/10.1021/acs.macromol.8b01597).
- 18 H. R. Kricheldorf, Syntheses of Biodegradable and Biocompatible Polymers by Means of Bismuth Catalysts, *Chem. Rev.*, 2009, **109**(11), 5579–5594, DOI: [10.1021/cr900029e](https://doi.org/10.1021/cr900029e).
- 19 S. E. Paramonov, E. M. Bachelder, T. T. Beaudette, S. M. Standley, C. C. Lee, J. Dashe and J. M. J. Fréchet, Fully Acid-Degradable Biocompatible Polyacetal Microparticles for Drug Delivery, *Bioconjug. Chem.*, 2008, **19**(4), 911–919, DOI: [10.1021/bc7004472](https://doi.org/10.1021/bc7004472).
- 20 O. Shelef, S. Gnaim and D. Shabat, Self-Immobilative Polymers: An Emerging Class of Degradable Materials with Distinct Disassembly Profiles, *J. Am. Chem. Soc.*, 2021, **143**(50), 21177–21188, DOI: [10.1021/jacs.1c11410](https://doi.org/10.1021/jacs.1c11410).
- 21 Y. Liang, H. Sun, W. Cao, M. P. Thompson and N. C. Gianneschi, Degradable Polyphosphoramidate via Ring-Opening Metathesis Polymerization, *ACS Macro Lett.*, 2020, **9**(10), 1417–1422, DOI: [10.1021/acsmacrolett.0c00401](https://doi.org/10.1021/acsmacrolett.0c00401).



22 C. C. Song, F. S. Du and Z. C. Li, Oxidation-Responsive Polymers for Biomedical Applications, *J. Mater. Chem. B*, 2014, 2(22), 3413–3426, DOI: [10.1039/c3tb21725f](https://doi.org/10.1039/c3tb21725f).

23 L. Wang, K. Zhu, W. Cao, C. Sun, C. Lu and H. Xu, ROS-Triggered Degradation of Selenide-Containing Polymers Based on Selenoxide Elimination, *Polym. Chem.*, 2019, 10(16), 2039–2046, DOI: [10.1039/c9py00171a](https://doi.org/10.1039/c9py00171a).

24 K. A. Miller, E. G. Morado, S. R. Samanta, B. A. Walker, A. Z. Nelson, S. Sen, D. T. Tran, D. J. Whitaker, R. H. Ewoldt, P. V. Braun, *et al.*, Acid-Triggered, Acid-Generating, and Self-Amplifying Degradable Polymers, *J. Am. Chem. Soc.*, 2019, 141(7), 2838–2842, DOI: [10.1021/jacs.8b07705](https://doi.org/10.1021/jacs.8b07705).

25 Y. Xu, S. Sen, Q. Wu, X. Zhong, R. H. Ewoldt and S. C. Zimmerman, Base-Triggered Self-Amplifying Degradable Polyurethanes with the Ability to Translate Local Stimulation to Continuous Long-Range Degradation, *Chem. Sci.*, 2020, 11(12), 3326–3331, DOI: [10.1039/c9sc06582b](https://doi.org/10.1039/c9sc06582b).

26 G. I. Peterson, D. C. Church, N. A. Yakelis and A. J. Boydston, 1,2-Oxazine Linker As a Thermal Trigger for Self-Immulative Polymers, *Polymer*, 2014, 55(23), 5980–5985, DOI: [10.1016/j.polymer.2014.09.048](https://doi.org/10.1016/j.polymer.2014.09.048).

27 G. R. Kiel, D. J. Lundberg, E. Prince, K. E. L. Husted, A. M. Johnson, V. Lensch, S. Li, P. Shieh and J. A. Johnson, Cleavable Comonomers for Chemically Recyclable Polystyrene: A General Approach to Vinyl Polymer Circularity, *J. Am. Chem. Soc.*, 2022, 144(28), 12979–12988, DOI: [10.1021/jacs.2c05374](https://doi.org/10.1021/jacs.2c05374).

28 Y. Lin, T. B. Kouznetsova and S. L. Craig, Mechanically Gated Degradable Polymers, *J. Am. Chem. Soc.*, 2020, 142(5), 2105–2109, DOI: [10.1021/jacs.9b13359](https://doi.org/10.1021/jacs.9b13359).

29 M. C. Parrott, J. C. Luft, J. D. Byrne, J. H. Fain, M. E. Napier and J. M. Desimone, Tunable Bifunctional Silyl Ether Cross-Linkers for the Design of Acid-Sensitive Biomaterials, *J. Am. Chem. Soc.*, 2010, 132(50), 17928–17932, DOI: [10.1021/ja108568g](https://doi.org/10.1021/ja108568g).

30 J. Szychowski, A. Mahdavi, J. J. L. Hodas, J. D. Bagert, J. T. Ngo, P. Landgraf, D. C. Dieterich, E. M. Schuman and D. A. Tirrell, Cleavable Biotin Probes for Labeling of Biomolecules via Azide-Alkyne Cycloaddition, *J. Am. Chem. Soc.*, 2010, 132(51), 18351–18360, DOI: [10.1021/ja1083909](https://doi.org/10.1021/ja1083909).

31 C. M. Bunton, Z. M. Bassampour, J. M. Boothby, A. N. Smith, J. V. Rose, D. M. Nguyen, T. H. Ware, K. G. Csaky, A. R. Lippert, N. V. Tsarevsky, *et al.*, Degradable Silyl Ether-Containing Networks from Trifunctional Thiols and Acrylates, *Macromolecules*, 2020, 53(22), 9890–9900, DOI: [10.1021/acs.macromol.0c01967](https://doi.org/10.1021/acs.macromol.0c01967).

32 M. C. Parrott, M. Finniss, J. C. Luft, A. Pandya, A. Gullapalli, M. E. Napier and J. M. Desimone, Incorporation and Controlled Release of Silyl Ether Prodrugs from PRINT Nanoparticles, *J. Am. Chem. Soc.*, 2012, 134(18), 7978–7982, DOI: [10.1021/ja301710z](https://doi.org/10.1021/ja301710z).

33 T. Ware, A. R. Jennings, Z. S. Bassampour, D. Simon, D. Y. Son and W. Voit, Degradable, Silyl Ether Thiol-Ene Networks, *RSC Adv.*, 2014, 4(75), 39991–40002, DOI: [10.1039/c4ra06997h](https://doi.org/10.1039/c4ra06997h).

34 S. Zhang, X. Q. Xu, S. Liao, Q. Pan, X. Ma and Y. Wang, Controllable Degradation of Polyurethane Thermosets with Silaketal Linkages in Response to Weak Acid, *ACS Macro Lett.*, 2022, 11(7), 868–874, DOI: [10.1021/acsmacrolett.2c00204](https://doi.org/10.1021/acsmacrolett.2c00204).

35 K. E. L. Husted, C. M. Brown, P. Shieh, I. Kevlishvili, S. L. Kristufek, H. Zafar, J. V. Accardo, J. C. Cooper, R. S. Klausen, H. J. Kulik, *et al.*, Remolding and Deconstruction of Industrial Thermosets via Carboxylic Acid-Catalyzed Bifunctional Silyl Ether Exchange, *J. Am. Chem. Soc.*, 2023, 145(3), 1916–1923, DOI: [10.1021/jacs.2c11858](https://doi.org/10.1021/jacs.2c11858).

36 K. E. L. Husted, P. Shieh, D. J. Lundberg, S. L. Kristufek and J. A. Johnson, Molecularly Designed Additives for Chemically Deconstructable Thermosets without Compromised Thermomechanical Properties, *ACS Macro Lett.*, 2021, 10(7), 805–810, DOI: [10.1021/acsmacrolett.1c00255](https://doi.org/10.1021/acsmacrolett.1c00255).

37 P. Shieh, W. Zhang, K. E. L. Husted, S. L. Kristufek, B. Xiong, D. J. Lundberg, J. Lem, D. Veysset, Y. Sun, K. A. Nelson, *et al.*, Cleavable Comonomers Enable Degradable, Recyclable Thermoset Plastics, *Nature*, 2020, 583(7817), 542–547, DOI: [10.1038/s41586-020-2495-2](https://doi.org/10.1038/s41586-020-2495-2).

38 Y. AlFaraj, S. Mohapatra, P. Shieh, K. Husted, D. Ivanoff, E. Lloyd, J. Cooper, Y. Dai, A. Singhal, J. Moore, *et al.*, A Model Ensemble Approach Enables Data-Driven Property Prediction for Chemically Deconstructable Thermosets in the Low Data Regime, *ChemRxiv*, 2023, 1–19.

39 P. Shieh, H. V. T. Nguyen and J. A. Johnson, Tailored Silyl Ether Monomers Enable Backbone-Degradable Polynorbornene-Based Linear, Bottlebrush and Star Copolymers through ROMP, *Nat. Chem.*, 2019, 11(12), 1124–1132, DOI: [10.1038/s41557-019-0352-4](https://doi.org/10.1038/s41557-019-0352-4).

40 A. M. Johnson, K. E. L. Husted, L. J. Kilgallon and J. A. Johnson, Orthogonally Deconstructable and Depolymerizable Polysilylethers via Entropy-Driven Ring-Opening Metathesis Polymerization, *Chem. Commun.*, 2022, 58(61), 8496–8499, DOI: [10.1039/d2cc02718f](https://doi.org/10.1039/d2cc02718f).

41 E. M. Lloyd, J. C. Cooper, P. Shieh, D. G. Ivanoff, N. A. Parikh, E. B. Mejia, K. E. L. Husted, L. C. Costa, N. R. Sottos, J. A. Johnson, *et al.*, Efficient Manufacture, Deconstruction, and Upcycling of High-Performance Thermosets and Composites, *ACS Appl. Eng. Mater.*, 2023, 1(1), 477–485, DOI: [10.1021/acsaenm.2c00115](https://doi.org/10.1021/acsaenm.2c00115).

42 R. A. Smith, G. Fu, O. McAteer, M. Xu and W. R. Gutekunst, Radical Approach to Thioester-Containing Polymers, *J. Am. Chem. Soc.*, 2019, 141(4), 1446–1451, DOI: [10.1021/jacs.8b12154](https://doi.org/10.1021/jacs.8b12154).

43 E. A. Prebihalo, A. M. Luke, Y. Reddi, C. J. LaSalle, V. M. Shah, C. J. Cramer and T. M. Reineke, Radical Ring-Opening Polymerization of Sustainably-Derived Thionoisochromanone, *Chem. Sci.*, 2023, 5689–5698, DOI: [10.1039/d2sc06040j](https://doi.org/10.1039/d2sc06040j).

44 G. Delaittre and L. Barner, The Para-Fluoro-Thiol Reaction as an Efficient Tool in Polymer Chemistry, *Polym. Chem.*, 2018, 9(20), 2679–2684, DOI: [10.1039/c8py00287h](https://doi.org/10.1039/c8py00287h).

45 P. Zhu, W. Meng and Y. Huang, Synthesis and Antibiofouling Properties of Crosslinkable Copolymers



Grafted with Fluorinated Aromatic Side Chains, *RSC Adv.*, 2017, **7**(6), 3179–3189, DOI: [10.1039/C6RA26409C](https://doi.org/10.1039/C6RA26409C).

46 C. Ott, R. Hoogenboom and U. S. Schubert, Post-Modification of Poly(Pentafluorostyrene): A Versatile “Click” Method to Create Well-Defined Multifunctional Graft Copolymers, *Chem. Commun.*, 2008, **30**, 3516–3518, DOI: [10.1039/b807152g](https://doi.org/10.1039/b807152g).

47 V. Atanasov and J. Kerres, Highly Phosphonated Polypentafluorostyrene, *Macromolecules*, 2011, **44**(16), 6416–6423, DOI: [10.1021/ma2011574](https://doi.org/10.1021/ma2011574).

48 J. M. Noy, A. K. Friedrich, K. Batten, M. N. Bhebhe, N. Busatto, R. R. Batchelor, A. Kristanti, Y. Pei and P. J. Roth, Para-Fluoro Postpolymerization Chemistry of Poly(Pentafluorobenzyl Methacrylate): Modification with Amines, Thiols, and Carbonylthiolates, *Macromolecules*, 2017, **50**(18), 7028–7040, DOI: [10.1021/acs.macromol.7b01603](https://doi.org/10.1021/acs.macromol.7b01603).

49 P. Boufflet, A. Casey, Y. Xia, P. N. Stavrinou and M. Heeney, Pentafluorobenzene End-Group as a Versatile Handle for Para Fluoro “Click” Functionalization of Polythiophenes, *Chem. Sci.*, 2017, **8**(3), 2215–2225, DOI: [10.1039/c6sc04427a](https://doi.org/10.1039/c6sc04427a).

50 S. Agar, E. Baysak, G. Hizal, U. Tunca and H. Durmaz, An Emerging Post-Polymerization Modification Technique: The Promise of Thiol-Para-Fluoro Click Reaction, *J. Polym. Sci. Part A Polym. Chem.*, 2018, **56**(12), 1181–1198, DOI: [10.1002/pola.29004](https://doi.org/10.1002/pola.29004).

51 Y. Pei, J. M. Noy, P. J. Roth and A. B. Lowe, Thiol-Reactive Passerini-Methacrylates and Polymorphic Surface Functional Soft Matter Nanoparticles *via* Ethanolic RAFT Dispersion Polymerization and Post-Synthesis Modification, *Polym. Chem.*, 2015, **6**(11), 1928–1931, DOI: [10.1039/c4py01558d](https://doi.org/10.1039/c4py01558d).

52 J. M. Noy, M. Koldevitz and P. J. Roth, Thiol-Reactive Functional Poly(Meth)Acrylates: Multicomponent Monomer Synthesis, RAFT (Co)Polymerization and Highly Efficient Thiol-Para-Fluoro Postpolymerization Modification, *Polym. Chem.*, 2015, **6**(3), 436–447, DOI: [10.1039/c4py01238k](https://doi.org/10.1039/c4py01238k).

53 C. S. Gudipati, C. M. Creenlief, J. A. Johnson, P. Prayonpan and K. L. Wooley, Hyperbranched Fluoropolymer and Linear Poly(Ethylene Glycol) Based Amphiphilic Crosslinked Networks as Efficient Antifouling Coatings: An Insight into the Surface Compositions, Topographies, and Morphologies, *J. Polym. Sci. Part A Polym. Chem.*, 2004, **42**(24), 6193–6208, DOI: [10.1002/pola.20466](https://doi.org/10.1002/pola.20466).

54 D. Gan, A. Mueller and K. L. Wooley, Amphiphilic and Hydrophobic Surface Patterns Generated from Hyperbranched Fluoropolymer/Linear Polymer Networks: Minimally Adhesive Coatings *via* the Crosslinking of Hyperbranched Fluoropolymers, *J. Polym. Sci. Part A Polym. Chem.*, 2003, **41**(22), 3531–3540, DOI: [10.1002/pola.10968](https://doi.org/10.1002/pola.10968).

55 P. M. Blackmore and W. J. Feast, Stereoregular Fluoropolymers: 6. The Ring-Opening Polymerization of N-Pentafluorophenylbicyclo[2.2.1]Hept-5-Ene-2,3-Dicarboximide, *J. Fluorine Chem.*, 1988, **40**(2–3), 331–347, DOI: [10.1016/S0022-1139\(00\)83072-9](https://doi.org/10.1016/S0022-1139(00)83072-9).

56 A. A. Santiago, J. Vargas, S. Fomine, R. Gavino and M. A. Tlenkopatchev, Polynorbornene with Pentafluorophenyl Imide Side Chain Groups: Synthesis and Sulfonation, *J. Polym. Sci. Part A Polym. Chem.*, 2010, **48**, 2925–2933.

57 Y. Xia, Y. Li, A. O. Burts, M. F. Ottaviani, D. A. Tirrell, J. A. Johnson, N. J. Turro and R. H. Grubbs, EPR Study of Spin Labeled Brush Polymers in Organic Solvents, *J. Am. Chem. Soc.*, 2011, **133**(49), 19953–19959, DOI: [10.1021/ja2085349](https://doi.org/10.1021/ja2085349).

58 H. V. T. Nguyen, A. Detappe, N. M. Gallagher, H. Zhang, P. Harvey, C. Yan, C. Mathieu, M. R. Golder, Y. Jiang, M. F. Ottaviani, *et al.*, Triply Loaded Nitroxide Brush-Arm Star Polymers Enable Metal-Free Millimetric Tumor Detection by Magnetic Resonance Imaging, *ACS Nano*, 2018, **12**(11), 11343–11354, DOI: [10.1021/acsnano.8b06160](https://doi.org/10.1021/acsnano.8b06160).

59 M. R. Golder, J. Liu, J. N. Andersen, M. V. Shipitsin, F. Vohidov, H. V. T. Nguyen, D. C. Ehrlich, S. J. Huh, B. Vangamudi, K. D. Economides, *et al.*, Reduction of Liver Fibrosis by Rationally Designed Macromolecular Telmisartan Prodrugs, *Nat. Biomed. Eng.*, 2018, **2**(11), 822–830, DOI: [10.1038/s41551-018-0279-x](https://doi.org/10.1038/s41551-018-0279-x).

60 F. Vohidov, J. N. Andersen, K. D. Economides, M. V. Shipitsin, O. Burenkova, J. C. Ackley, B. Vangamudi, H. V. T. Nguyen, N. M. Gallagher, P. Shieh, *et al.*, Design of BET Inhibitor Bottlebrush Prodrugs with Superior Efficacy and Devoid of Systemic Toxicities, *J. Am. Chem. Soc.*, 2021, **143**(12), 4714–4724, DOI: [10.1021/jacs.1c00312](https://doi.org/10.1021/jacs.1c00312).

61 A. Detappe, H. V. T. Nguyen, Y. Jiang, M. P. Agius, W. Wang, C. Mathieu, N. K. Su, S. L. Kristufek, D. J. Lundberg, S. Bhagchandani, *et al.*, Molecular Bottlebrush Prodrugs as Mono- and Triplex Combination Therapies for Multiple Myeloma, *Nat. Nanotechnol.*, 2023, **18**(2), 184–192, DOI: [10.1038/s41565-022-01310-1](https://doi.org/10.1038/s41565-022-01310-1).

62 S. H. Bhagchandani, F. Vohidov, L. E. Milling, E. Y. Tong, C. M. Brown, M. L. Ramseier, B. Liu, T. B. Fessenden, H. V. T. Nguyen, G. R. Kiel, *et al.*, Engineering Kinetics of TLR7/8 Agonist Release from Bottlebrush Prodrugs Enables Tumor-Focused Immune Stimulation, *Sci. Adv.*, 2023, **9**(16), eadg2239, DOI: [10.1126/sciadv.adg2239](https://doi.org/10.1126/sciadv.adg2239).

63 H. Turgut, A. C. Schmidt, P. Wadhwan, A. Welle, R. Müller and G. Delaittre, The Para-Fluoro-Thiol Ligation in Water, *Polym. Chem.*, 2017, **8**(8), 1288–1293, DOI: [10.1039/c6py02108e](https://doi.org/10.1039/c6py02108e).

64 E. P. Serjeant, B. Dempsey, *Ionisation constants of organic acids in aqueous solution* Pergamon Press, Oxford, 1979.

65 S. Kovačić and C. Slugovc, Ring-Opening Metathesis Polymerisation Derived Poly(Dicyclopentadiene) Based Materials, *Mater. Chem. Front.*, 2020, **4**(8), 2235–2255, DOI: [10.1039/d0qm00296h](https://doi.org/10.1039/d0qm00296h).

